Effects of Polydispersity on the Order−Disorder Transition in Block Copolymer Melts

Nathaniel A. Lynd and Marc A. Hillmyer*

Department of Chemistry, University of Minnesota, 207 Pleasant St. SE, Minneapolis, Minnesota 55455-0431

Received April 25, 2007; Revised Manuscript Received July 27, 2007

ABSTRACT: We prepared controlled-polydispersity poly(ethylene-*alt*-propylene)-*b*-poly(DL-lactide) (PL) and polystyrene-*b*-polyisoprene (SI) block copolymers to study the effects of the molecular weight distribution on the order−disorder transition at controlled composition and overall molecular weight. Small-angle X-ray scattering and rheological measurements were carried out to characterize the changes in the order−disorder transition in these self-assembled materials as a function of their composition and polydispersity index. We determined that in both asymmetric PL and SI systems increasing polydispersity in the minority component resulted in a decrease in the segregation strength at the order−disorder transition, whereas increasing polydispersity in the majority component results in an increase in the segregation strength at the order−disorder transition. We speculate that increasing PDI in the majority domain weakens the effective potential holding the phase-separated microdomains ordered on a lattice.

Introduction

Immiscible polymers engaged by a covalent bond at their termini form the basis for a versatile class of self-assembling materials: block copolymers. Much attention has been focused both experimentally and theoretically on elucidating the full complexity and underlying physical phenomena that dictate their self-assembly. To date, most of those efforts have utilized or focused on materials with narrow distributions in their molecular weight, i.e., as manifest by polydispersity indices (PDI = M_w/M_n) that approach 1.

The effects of polydispersity on the self-assembly of diblock copolymers have received little experimental attention.[1−3] This is in contrast to the numerous notable theoretical treatments spanning the past two decades beginning with Leibler and Benoit[4] and Hong and Noolandi,[5] who treated disordered block copolymer melts. Most recently, Cooke and Shi[6] treated both disordered and ordered diblock copolymer melts at low levels of polydispersity by approximating observable quantities as a Taylor series expansion about the average molecular weight; this efficient technique allowed for examination of the effects of PDI increasing asymmetrically in one block in a similar manner to Sides and Fredrickson[10] or symmetrically in both blocks in a similar manner to Burger et al.[7] at weak segregation. However, Cooke and Shi were only able to calculate relevant observables at modest levels of polydispersity ($PDI_A \leq 1.2$). Nonetheless, qualitative agreement was found where experimental data were available.[3,8] Domain spacing increased as the PDI was increased, and PDI increases in one block of an asymmetric diblock copolymer resulted in transitions to morphologies with increased mean interfacial curvature toward that block.

Theoretical treatment of polydispersity effects in diblock copolymer melts near the order−disorder transition (ODT)[9] have been accomplished using the random-phase approximation (RPA) and self-consistent mean-field theory.[4−7,10,24,29] To date, there has been no experimental evidence to support or refute the general prediction that as PDI increases, the segregation strength required at the ODT, $(\chi N)_{ODT}$, decreases. For example, using the RPA[4−7,10] at $f_A = 0.5$, $(\chi N)_{ODT} \approx 10.5$ in the monodisperse limit, at a $PDI_A = 2.0$ ($PDI_B = 1$), $(\chi N)_{ODT} \approx 7.4$.[4−7,10] For typical block copolymers ($\chi \propto T^{-1}$) this decrease in $(\chi N)_{ODT}$ would lead to an increase in the temperature required to bring about a disordered state, the magnitude of which would depend on the exact temperature dependence of χ.

The effects of PDI on the ODT have potential implications on the processability of block copolymers. In general, processing is best carried out above the ODT;[11] the tuning of the block copolymer PDI could serve as a convenient means to change the location of the ODT, potentially to bring a block copolymer system under more favorable processing conditions. From a more fundamental viewpoint, experiments examining the ODT are of utmost interest since this is the region believed most likely to disagree with these mean-field theory predictions,[12] particularly as the molecular weights of the block copolymers are decreased.[13] Utilizing two different controlled-polydispersity block copolymer systems—poly(ethylene-*alt*-propylene)-*b*-poly(DL-lactide) (PL) and polystyrene-*b*-polyisoprene (SI), we systematically explore the effects of polydispersity on the order−disorder transition.

Results

Synthesis of Controlled Polydispersity Block Copolymer Materials. The synthesis of controlled-polydispersity PL materials has been discussed in detail elsewhere.[8,20] SI was synthesized using anionic polymerization to yield materials with variable polydispersity indices (PDIs) in the polystyrene block. This was accomplished through the metered addition of a dilute solution of *sec*-butyllithium initiator by syringe pump to a rapidly stirring solution of styrene monomer in cylcohexane at 30−45 °C. Initiation by this method has the effect of simulating a slow rate of initiation relative to propagation, thus increasing the PDI of the polystyrene. The PDI of the polydisperse block was fine-tuned by altering the reaction temperature; a higher reaction temperature resulted in a larger PDI. PDI can be related to the ratio of the propagation and initiation rate constants (k_p/

* To whom correspondence should be addressed. E-mail: hillmyer@chem.umn.edu.

10.1021/ma070962r CCC: $37.00
Published on Web 10/04/2007

Table 1. Molecular and Morphological Characteristics of the Diblock Copolymers

sample ID	N_{total}[a]	f_{PDI}[b]	PDI[c]	PDI[d]	morphology[e]	T_{ODT} (K)[f]	σ_T	$(\chi N)_{ODT}$[g]
PL(0.34,1.18)-1	37.2	0.344	1.18	1.08	L	487	1.3	10.1
PL(0.34,1.37)-1	36.9	0.339	1.37	1.15	G	493	1.4	9.65
PL(0.33,1.43)-1	36.2	0.326	1.43	1.17	C	500	1.6	9.07
PL(0.31,1.89)-1	35.5	0.313	1.89	1.17	C	499	1.5	8.97
PL(0.31,2.05)-1	35.5	0.313	2.05	1.20	C	495	1.7	9.15
PL(0.50,1.36)-2	25.9	0.494	1.36	1.15	L	442	0.2	9.04
PL(0.48,1.35)-2	25.1	0.478	1.35	1.14	L	440	0.3	8.89
PL(0.47,1.45)-2	24.8	0.472	1.45	1.17	L	438	0.3	8.85
PL(0.49,1.49)-2	25.5	0.486	1.49	1.19	L	444	0.1	8.81
PL(0.47,1.61)-2	24.6	0.467	1.61	1.22	L	436	0.4	8.86
PL(0.46,1.82)-2	24.1	0.459	1.82	1.28	L	441	0.1	8.51
PL(0.46,1.82)-2	24.2	0.459	1.82	1.28	L	443	0.3	8.42
PL(0.54,1.22)-3	26.1	0.498	1.22	1.11	L	448	1.3	9.63
PL(0.55,1.32)-3	26.7	0.509	1.32	1.15	L	449	1.7	9.82
PL(0.55,1.35)-3	26.5	0.506	1.35	1.16	L	440	1.6	10.2
PL(0.55,1.45)-3	26.8	0.511	1.45	1.20	L	450	0.8	9.78
PL(0.54,1.72)-3	26.3	0.502	1.72	1.31	L	453	1.7	9.43
PL(0.53,2.00)-3	25.6	0.488	2.00	1.41	L	451	1.7	9.27
PL(0.59,1.20)-4	31.9	0.589	1.20	1.11	G	439	0.6	11.3
PL(0.58,1.23)-4	31.5	0.584	1.23	1.12	G	439	4.3	11.2
PL(0.59,1.73)-4	32.1	0.592	1.73	1.36	L	442	0.6	11.2
PL(0.59,1.85)-4	31.9	0.589	1.85	1.41	L	446	1.3	10.9
PL(0.62,1.30)-5	34.4	0.619	1.30	1.16	G	441	1.4	12.1
PL(0.61,1.32)-5	33.1	0.604	1.32	1.17	G	444	3.2	11.4
PL(0.61,1.33)-5	33.5	0.609	1.33	1.17	G	442	3.0	11.7
PL(0.62,1.39)-5	34.2	0.617	1.39	1.21	G	449	0.3	11.5
PL(0.62,1.62)-5	34.3	0.618	1.62	1.32	L	438	0.4	12.2
PL(0.63,1.42)-6	35.6	0.632	1.42	1.23	C	447	1.5	12.1
PL(0.64,1.42)-6	36.8	0.644	1.42	1.23	C	455	0.2	12.0
PL(0.63,1.57)-6	35.6	0.632	1.57	1.30	G	427	0.8	13.5
PL(0.64,1.67)-6	36.7	0.643	1.67	1.36	G	424	0.2	14.1
SI(0.29,1.07)-7	291	0.287	1.07	1.05	C	420	0.6	24.6
SI(0.29,1.13)-7	239	0.288	1.13	1.05	C	398	0.1	22.4
SI(0.30,1.15)-7	240	0.295	1.15	1.07	C	411	1.4	21.1
SI(0.52,1.21)-8	365	0.516	1.21	1.21	L	523	0.7	18.6
SI(0.51,1.29)-8	345	0.507	1.29	1.16	L	524	0.1	17.4
SI(0.50,1.34)-8	369	0.501	1.34	1.19	L	546	3.1	16.6
SI(0.64,1.04)-9	223	0.640	1.04	1.06	G	433	0.6	17.7
SI(0.64,1.12)-9	238	0.643	1.12	1.10	P[15]	441	0.6	18.2
SI(0.65,1.25)-9	217	0.649	1.25	1.14	L	421	0.0	18.3

[a] Determined by ^{1}H NMR spectroscopy, the densities at room temperature ($\rho_{PEP} = 0.856$,[16] $\rho_{PLA} = 1.265$,[17] $\rho_{PS} = 1.05$, $\rho_{PI} = 0.90$[21]), and with reference to a segment volume ($v_{ref} = 144$ Å^3). [b] The composition of the polydisperse component, $f_{PDI} = N_{PDI}/(N_{PDI} + N_{MONO})$, where N_{PDI} is the number of segments in the polydisperse block and N_{MONO} is the number of segments in the monodisperse block. [c] Polydispersity index of the PLA as calculated[8] or PS block as measured by RI-SEC using THF as the mobile phase at 40 °C relative to PS standards. [d] Polydispersity index of the PEP−PLA or PS−PI block copolymer as measured by RI-SEC using THF as the mobile phase at 40 °C relative to PS standards. [e] Morphology immediately before disordering as identified by SAXS (L = lamellar, G = gyroid, C = hexagonally packed cylinders, P = perforated lamellae). [f] Measured by DMA. For the PL samples this value represents the average of six measurements (three heating, three cooling, 1−3 °C/min) of the ODT; the error (σ_T) is the standard deviation of those measurements. For the SI samples, this value represents the average of three heating measurements (1−3 °C/min); the error is the standard deviation. [g] T_{ODT} converted to $(\chi N)_{ODT}$ using literature temperature-dependent expressions for the interaction parameter per segment, $\chi_{PEP-PLA}$ and χ_{PS-PI}, and the number of segments with respect to the appropriate segment volume (N_{total}). The error ($\sigma_{\chi N}$) was calculated by $\sigma_{\chi N} = \alpha/T_{ODT}^2\sigma_T$ with $\alpha = 71.4$ for PS−PI and $\alpha = 333.3$ for PEP−PLA; these parameters are from the temperature-dependent expression for the interaction parameter per segment (eqs 1 and 2). In all cases, $\sigma_{\chi N} < 0.3$.

k_i), and if the activation energy for initiation is lower than that for propagation, then k_p/k_i will decrease with increasing temperature.[14] Thus, in general one would expect a higher PDI at higher temperature. Once the styrene monomer was consumed, isoprene monomer was added to the reaction at once resulting in PS−PI with low PDIs in the PI block.[30]

The relevant molecular and morphological details of the PL and SI materials are summarized in Table 1. Each sample is identified by its sample name beginning with PL or SI for PEP−PLA or PS−PI, respectively, followed by the fractional composition of the polydisperse component (the PLA block for the PL samples and the PS block for the SI samples) and its polydispersity in parentheses. This code is followed by an integer to indicate to which series the sample belongs, e.g., SI-(0.64,1.04)-9 denotes a PS−PI block copolymer with $f_{PS} = 0.64$ and $PDI_{PS} = 1.04$, which belongs to series 9. There are six series of PEP−PLA diblock copolymers and three series of PS−PI diblock copolymers, each in a different composition window. The composition range for a particular series is generally narrow (ca. 0.01).

Size-exclusion chromatographs of the polystyrene blocks of SI(0.64,1.04)-9, SI(0.64,1.12)-9, and SI(0.65,1.25)-9 are shown in Figure 1. SI(0.64,1.04)-9 was polymerized by adding the *sec*-butyllithium solution rapidly, thus essentially initiating all chains simultaneously at 40 °C. SI(0.64,1.12)-9 and SI(0.65,1.25)-9 were prepared by adding the *sec*-butyllithium solution over a 31 min time period at a linearly increasing rate of addition at 38.5 and 45 °C, respectively; these two protocols resulted in differing breadths in their molecular weight distributions.

Effects of Increased Polydispersity on the ODT. The order−disorder transitions of all samples were measured rheologically by dynamic temperature sweeps in the linear viscoelastic regime and verified by small-angle X-ray scattering, as shown in Figure 2. The order−disorder temperature (T_{ODT})

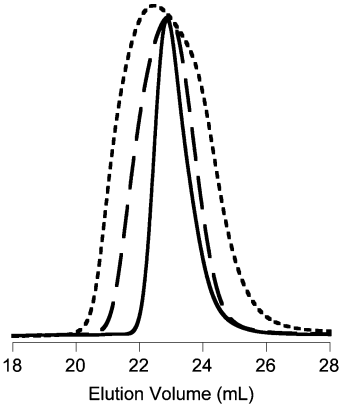

Figure 1. RI-SEC traces of the PS blocks of SI(0.64,1.04)-9 (solid), SI(0.64,1.12)-9 (dashed), and SI(0.65,1.25)-9 (dotted) with M_n = 13 010, 13 930, and 12 580 g mol^{-1}, respectively.

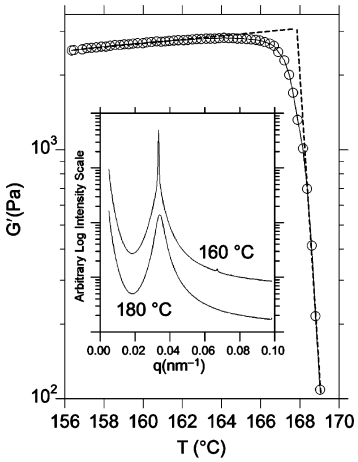

Figure 2. Measurement of the order−disorder transition was carried out by rheological and small-angle X-ray scattering measurements. The method of locating the ODT of SI(0.64,1.12)-9 is depicted in this figure as the intersection of the two extrapolated lines: T_{ODT} = 168 °C (1 °C/min). The inset shows the corresponding SAXS data at 160 and 180 °C.

was identified by a precipitous drop in low-frequency storage modulus (G') over a small temperature increment.[18] Specifically, the T_{ODT} was identified by a double extrapolation as shown in Figure 2 and recorded as the intersection of the two extrapolated lines; this method has proven very reproducible (see σ_T in Table 1). As evidence that the change in modulus was due to the loss of microstructural order in the sample, SAXS profiles of the principal scattering peak at 160 and 180 °C are also shown for this specific sample. The loss of order upon heating above the T_{ODT} is evident by the disappearance of higher order reflections and a discontinuous decrease in the intensity of the primary reflection.[19]

The T_{ODT} values could be converted to $(\chi N)_{ODT}$, the segregation strength at the ODT, using previously determined, temperature-dependent expressions for the segment−segment interaction parameters for PEP−PLA[20] and PS−PI[21,22] with respect to a reference volume of 144 Å^3:

$$\chi_{PEP-PLA}(T) = \frac{333}{T} - 0.44 \quad (1)$$

$$\chi_{PS-PI}(T) = \frac{71.4}{T} - 0.086 \quad (2)$$

$(\chi N)_{ODT}$ vs PDI of the PLA block for the PEP−PLA diblock copolymers, series 1−6 in Table 1, are shown in Figure 3. Each

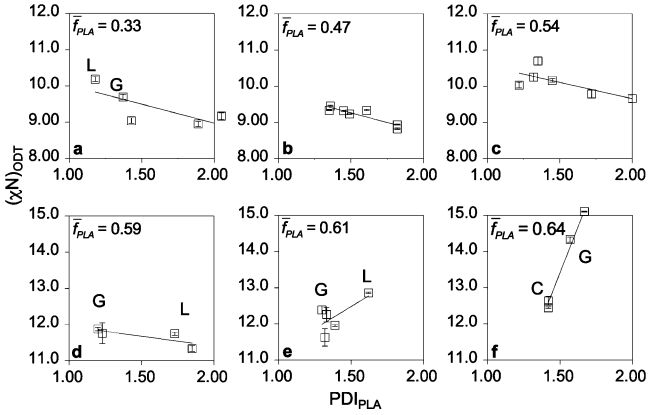

Figure 3. $(\chi N)_{ODT}$ vs PDI of the polydisperse PLA block. Data are fit to a line as a guide to the eye. (a) Series 1: $\bar{f}_{PLA}$ = 0.33; all samples were C immediately before the ODT except where noted. One point lies outside the boundary of the plot but is included in the fit. (b) Series 2: $\bar{f}_{PLA}$ = 0.47; all samples L. (c) Series 3: $\bar{f}_{PLA}$ = 0.54; all samples L. (d) Series 4: $\bar{f}_{PLA}$ = 0.59; morphologies indicated on plot. (e) Series 5: $\bar{f}_{PLA}$ = 0.61; morphologies indicated on plot. (f) Series 6: $\bar{f}_{PLA}$ = 0.64; morphologies indicated on plot; one point lies outside the boundary of the plot but is included in the fit.

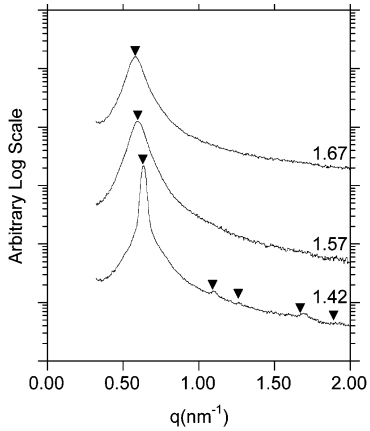

Figure 4. SAXS profiles at 160 °C ($\chi N \approx 13.2$) of series 6, $\bar{f}_{PLA}$ = 0.64. PDI of the PLA block is indicated to the right of each scattering profile. The sequence of profiles highlights the decrease in scattered intensity as the PDI is increased.

plot (a−f) is a depiction of the trend for a series of diblock copolymers that possess approximately equivalent composition and overall N (molecular weight) (see Table 1). Each data point is the average of six measurements of T_{ODT}, and the error bars represent the standard deviation about the mean (see Table 1).

In plots a−d, the slope of a line fit to the data is negative. It should be noted that this is in qualitative agreement with mean-field theory predictions that as the PDI increases, $(\chi N)_{ODT}$ should decrease.[4−7,10] This infers that the ordered state is stabilized with respect to the disordered state as PDI is increased at these compositions. In plots e and f the trend reverses; as the PDI increases, $(\chi N)_{ODT}$ appears to increase. This is in qualitative disagreement with previous self-consistent mean-field theory (SCFT) calculations which predict that although the decrease in $(\chi N)_{ODT}$ as PDI is increased in the majority block should be less pronounced than when the PDI increased in the minority block, it should nevertheless decrease as PDI is increased.[6,10] Morphological transitions often occurred within a single series; i.e., within each series, the ODT does not always occur between a *single* morphology and the disordered state. The morphologies of the ordered states prior to disorder are indicated in Figure 3.

Figure 4 shows the small-angle X-ray scattering at 160 °C ($\chi N \approx 13.2$) for three samples of series 6 shown in Figure 3f.

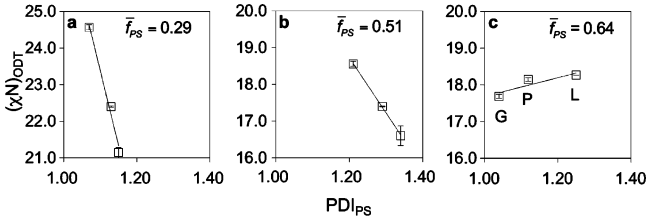

Figure 5. $(\chi N)_{ODT}$ vs PDI of the polydisperse PS block. (a) Series 7: $\bar{f}_{PS} = 0.29$; all samples exhibit the C morphology immediately before the ODT. (b) Series 8: $\bar{f}_{PS} = 0.54$; all samples exhibit the L morphology immediately before the ODT. (c) Series 9: $\bar{f}_{PS} = 0.64$; samples exhibit the indicated morphology prior to the ODT.

The system undergoes a transition from an ordered hexagonally packed cylindrical state at PDI = 1.42 of the polydisperse block to a disordered state at PDI = 1.57. Upon a further PDI increase the disordered state scattering intensity appears to decrease as the system moves farther from its ordering transition. This is in qualitative contradiction with mean-field theory predictions for the disordered state scattering that as PDI independently increases in the majority block, the system should near its ordering transition which would be accompanied by an increase in the scattering intensity.[4−7,10]

The effects of PDI on the ODT utilizing PS−PI, a block copolymer of a different chemical identity and higher overall molecular weight than the PL system, were also investigated. The ODT measurements for the nine SI samples in Table 1 are shown in Figure 5, plots a−c. The plots are presented in increasing fractional composition of the PS block. At $f_{PS} = 0.29$ (plot a) a strongly decreasing trend is observed over a small range in PDI. At $f_{PS} = 0.54$ (plot b) a decreasing trend is also observed however with a smaller dependence on PDI. Finally, at $f_{PS} = 0.64$ (plot c), the trend appears to reverse itself and $(\chi N)_{ODT}$ increases slightly as PDI is increased. These changes in the dependence of $(\chi N)_{ODT}$ on PDI are consistent with the behavior observed in the PEP−PLA system. The samples in this series exhibit different morphologies as well in a manner that is consistent with theory and previous experimental results; i.e., increasing PDI in the majority component of an asymmetric diblock copolymer promotes transitions toward morphologies with decreased mean interfacial curvature.[6,8] It should be noted that one of the samples (SI(0.64,1,12)-9) exhibited a morphology most consistent with the metastable perforated lamellar structure upon cooling from the disordered state.[23]

Discussion

The changes in the ODT as polydispersity is changed have been measured in two different block copolymer systems: PL and SI. A consistent trend between these two sets of molecules has emerged. In asymmetric diblock copolymers of PL and SI, increasing PDI in the minority block leads to decreased $(\chi N)_{ODT}$ (Figure 3a,b and Figure 5a). We attribute this stabilization of the ordered state relative to the disordered state as PDI is increased to a decreased entropic cost associated with filling space uniformly in the minority domains by the polydisperse component.[6,24] In a microphase-separated domain the wider distribution of chain lengths available at increased PDI leads to an overall decrease in the entropic stretching penalty, thus decreasing the free energy of the ordered state relative to the homogeneous disordered state. As shown before, increasing PDI in the minority component also favors transitions toward morphologies with increased interfacial curvature toward the polydisperse block.[8] For symmetric PL and SI, increasing PDI also led to decreased $(\chi N)_{ODT}$ (Figure 3b,c and Figure 5b).

In asymmetric diblock copolymers where the PDI is increased in the majority component, the opposite effect on the ODT was observed. As the PDI increases in the majority component, $(\chi N)_{ODT}$ increases (Figure 3e,f and Figure 5c). This represents a destabilization of the ordered state relative to the disordered state as the PDI of the majority block is increased. Contrary to the previous case, this is in disagreement with prior self-consistent mean-field theory (SCFT) calculations[6,10] which predict that $(\chi N)_{ODT}$ decreases as PDI is increased for all compositions of the polydisperse component.

We believe this discrepancy between theory[6,7,10] and experiment can be accounted for by considering a self-assembled mesophase to consist of block copolymer micelles ordered on a lattice. Increased polydispersity of the corona blocks decreases the entropic penalty of moving a micelle from its equilibrium position due to the greater number of chain lengths in the corona available to accommodate a random displacement. Thus, the free energy penalty of moving micelles from their equilibrium lattice positions is reduced.[25] This represents an effective decrease in the strength of the potential holding these micelles in their equilibrium lattice positions, bringing the system closer to an entropically favored disordered micellar state. Consistent with this hypothesis, Bendejacq et al. observed that highly asymmetric and polydisperse polystyrene-*b*-poly(acrylic acid) diblock copolymers in the melt state were characterized by disordered micellar arrangements of microdomains whereas the more symmetrical samples formed ordered assemblies.[1] We posit that stabilization of the ordered state over the disordered state due to the entropic gain associated with increased polydispersity in the majority domain is overwhelmed by the effects of effectively decreasing the strength of the interaction potential between the ordered micelles. High-resolution synchrotron SAXS experiments could be used to support this by exploring the nature of the disordered state near the ODT and potentially observe lattice melting occurring at the ODT.[26−28] As well, quantitative mechanical measurements may be able to detect any change in the modulus of the mesophase as polydispersity is increased provided that the samples exhibit the same ordered state morphology.

Recent SCFT calculations by Matsen present a more refined picture of the phase diagram for polydisperse block copolymers by including the close-packed spherical (S_{cp}) morphology and the possibility of macrophase separation.[29] The S_{cp} morphology encompasses a large region of the phase diagram, and significant two-phase regions are predicted as the PDI of one block is increased to 1.5. Furthermore, Matsen predicts ordered state destabilization in highly asymmetric polydisperse diblock copolymers. On the basis of this phase diagram, further experimentation may reveal that increasing the PDI at compositions less than $f_{PLA} = 0.33$ (or $f_{PS} = 0.29$) causes destabilization of the ordered state as it does for f_{PLA} (or f_{PS}) = 0.64.

Increasing PDI asymmetrically in a diblock copolymer yields changes in the ODT that depend on the diblock copolymer composition. This offers some freedom is changing the order−disorder transition temperature above which block copolymer materials are processed.[11] Specifically, the order−disorder transition temperature may be increased by increasing PDI in the minority component of a diblock copolymer; alternatively, the order−disorder transition temperature may be decreased by increasing PDI in the majority component.

Conclusion

The effects of increasing polydispersity on the order−disorder transition were investigated in poly(ethylene-*alt*-propylene)-*b*-

poly(DL-lactide) and polystyrene-*b*-polyisoprene by increasing the PDI in the poly(DL-lactide) and polystyrene blocks, while keeping the PDI constant in the poly(ethylene-*alt*-propylene) and polyisoprene blocks.[30] Typically, increasing PDI decreases $(\chi N)_{ODT}$ except when the PDI is increased in a block comprising the majority of the diblock copolymer, where $(\chi N)_{ODT}$ increases with increasing PDI. We account for this behavior by speculating that increasing PDI in the majority domain weakens the effective potential holding the phase-separated microdomains ordered on a lattice.

Experimental Section

Materials. All materials were used as received unless otherwise specified. Styrene (Aldrich) was degassed and stirred over CaH_2 (Aldrich) for several hours followed by vacuum distillation to a flask containing butylmagnesium chloride (Aldrich) where it was further degassed and allowed to stir for several hours at 0 °C before being transferred to a flame-dried and tared buret. Isoprene (Aldrich) was distilled twice from *n*-butyllithium (Aldrich, 2.5 M in hexanes) at 0 °C before being transferred to a flame-dried and tared buret. Cyclohexane was purified by passage through an activated alumina (LaRoche) column to remove protic impurities and a supported copper catalyst (Q-5 Engehardt) to remove trace amounts of oxygen.[31]

Synthesis of Poly(ethylene-*alt*-propylene)-*b*-poly(DL-lactide). The materials, reagents, conditions, and specific methods used to synthesize controlled-polydispersity PEP−PLA materials used in this study have been described in detail elsewhere.[8,20]

Synthesis of Controlled-Polydispersity Polystyrene-*b*-polyisoprene. To a flame-dried reactor fitted with Ace threads, a septum, and a Teflon-coated stir bar was attached a buret of purified styrene, isoprene, and cyclohexane under positive Ar(g) flow. The reactor was evacuated and filled with Ar(g) five times. Under static positive Ar(g) pressure, cyclohexane and styrene were added and warmed to 30−45 °C. A gastight syringe fitted with a long needle and filled with 0.8−2 mL of a dilute solution of *sec*-butyllithium was inserted into the reactor such that the needle extended into the styrene solution. The syringe was attached to a syringe pump, and the *sec*-butyllithium was added at a controlled and linearly increasing rate for typically 30 min. After 5 h the isoprene was added to the stirring polystyryl anion solution and allowed to react overnight. The reaction was terminated with a degassed 1:1 volume solution of isopropanol and methanol. The polystyrene-*b*-polyisoprene was precipitated in a 1:1 volume solution of isopropanol and methanol and collected by vacuum filtration. 0.2 wt % of BHT was added by codissolution in THF followed by evaporation and drying in vacuo.[21]

The polydispersity of the polystyrene block was changed by altering the rate of addition of *sec*-butyllithium and fine-tuned by changing the reaction temperature. In general, a polydispersity increase could be manifested either by decreasing the rate of addition of *sec*-butyllithium or by an increase in reaction temperature. The highest polydispersity index reached in this study was 1.34; however, obtaining higher values of the PDI by this method is theoretically possible.

Molecular Characterization. Molecular weights of SI and PL samples were determined by ^{1}H NMR spectroscopy at 500 MHz using a Varian Inova 500 spectrometer. Samples were dissolved in $CDCl_3$ (Cambridge Isotope Laboratories) at concentrations of about 1.0 wt %. 16 scans were taken per spectrum with a delay time of 10 s between consecutive pulses. PDI was determined using size exclusion chromatography (SEC) on a Hewlett-Packard 1100 series liquid chromatograph fitted with a Hewlett-Packard 1047A refractive index detector and three Jordi polydivinylbenzene columns with 10^4, 10^3, and 500 Å pore sizes and calibrated with polystyrene standards (Polymer Laboratories). Tetrahydrofuran was used as the mobile phase with a flow rate of 1 mL/min at 40 °C.

Small-Angle X-ray Scattering. Measurements were performed on the University of Minnesota Twin Cities Characterization Facility beamline. Cu Kα X-rays ($\lambda = 1.542$ Å) were generated by a Rigaku RU-200BVH rotating anode fitted with a 0.2×2 mm^2 microfocus cathode and Franks mirror optics. Temperature control inside the evacuated sample chamber was accomplished with water cooling and electrically heating the brass-block sample holder. Two-dimensional diffraction images were recorded using a Siemens area detector located at the end of a 2.30 or 1.04 m evacuated flight tube and corrected for detector response before analysis. SAXS measurements for the PS−PI samples were further carried out at the Advanced Photon Source (APS) on beamline 5 ID-D, which is maintained by the DuPont-Northwestern-Dow Collaborative Access Team (DND-CAT). The X-ray source operated at a wavelength of 0.83 Å with a sample-to-detector distance of 6.03 m calibrated with a laboratory standard. The scattered intensity was measured on a Mar 165 mm CCD X-ray detector at a resolution of 2048×2048. The two-dimensional images were azimuthally integrated and reduced to the one-dimensional form of scattered intensity vs the spatial frequency q.

Dynamic Mechanical Analysis. Dynamic strain, frequency, and temperature sweeps were carried out in a TA Instruments ARES rheometer with 25 or 8 mm parallel plate geometries using a 1 mm gap. Dynamic strain sweeps were carried out to identify the linear viscoelastic regime (0.1−1% strain). Dynamic temperature ramp tests were performed between 1 and 3 °C/min at a frequency of 1.0 rad/s. The elastic (G') and loss (G'') moduli were recorded as a function of temperature. The order−disorder temperature (T_{ODT}) was identified by a precipitous drop in storage modulus (G') over a small temperature increment and determined by the double-extrapolation method shown in Figure 2. The standard deviation in T_{ODT} was less than 4.3 K in all measurements (Table 1). This standard deviation is in part due to the hystereisis between heating and cooling temperature ramps in the PL samples and not actual error in the measurement.

Acknowledgment. This work was supported primarily by the MRSEC Program of the National Science Foundation under Award DMR-0212302. Portions of this work were performed at the DuPont-Northwestern-Dow Collaborative Access Team (DND-CAT) located at Sector 5 of the Advanced Photon Source (APS). DND-CAT is supported by E. I. Dupont de Nemours & Co., The Dow Chemical Company, and the State of Illinois. Use of the APS was supported by the U.S. Department of Energy, Office of Science, Office of Basic Energy Sciences, under Contract DE-AC02-06CH11357. The authors thank David C. Morse, Amit Ranjan, and Mark W. Matsen for helpful discussions. N.A.L. acknowledges support from the Graduate School at the University of Minnesota for a Doctoral Dissertation Fellowship.

References and Notes

(1) Bendejacq, D.; Ponsinet, V.; Joanicot, M.; Loo, Y.-L.; Register, R. A. *Macromolecules* **2002**, *35*, 6645.
(2) Ruzette, A.-V.; Tencé-Girault, S.; Leibler, L.; Chauvin, F.; Bertin, D.; Guerret, O.; Gérard, P. *Macromolecules* **2006**, *39*, 5804.
(3) Matsushita, Y.; Noro, A.; Iinuma, M.; Suzuki, J.; Ohtani, H.; Takano, A. *Macromolecules* **2003**, *36*, 8074. Noro, A.; Iinuma, M.; Suzuki, J.; Takano, A.; Matsushita, Y. *Macromolecules* **2004**, *37*, 3804. Noro, A.; Cho, D.; Takano, A.; Matsushita, Y. *Macromolecules* **2005**, *38*, 4371.
(4) Leibler, L.; Benoit, H. *Polymer* **1981**, *22*, 195.
(5) Hong, K. M.; Noolandi, J. *Polym. Commun.* **1984**, *25*, 265.
(6) Cooke, D. M.; Shi, A.-C. *Macromolecules* **2006**, *39*, 6661.
(7) Burger, C.; Ruland, W.; Semenov, A. N. *Macromolecules* **1990**, *23*, 3339. Burger, C.; Ruland, W.; Semenov, A. N. *Macromolecules* **1991**, *24*, 816.
(8) Lynd, N. A.; Hillmyer, M. A. *Macromolecules* **2005**, *38*, 8803.
(9) Rosedale, J. H.; Bates, F. S.; Almdal, K.; Mortensen, K.; Wignall, G. D. *Macromolecules* **1995**, *28*, 1429.
(10) Sides, S. W.; Frederickson, G. H. *J. Chem. Phys.* **2004**, *121*, 4974.
(11) Bates, F. S.; Fredrickson, G. H.; Hucul, D.; Hahn, S. F. *AIChE J.* **2001**, *47*, 762.
(12) Matsen, M. W. *J. Phys.: Condens. Matter* **2002**, *14*, R21.

(13) Fredrickson, G. H.; Helfand, E. *J. Chem. Phys.* **1987**, *87*, 697. Ganesan, V.; Fredrickson, G. H. *Europhys. Lett.* **2001**, *55*, 814.
(14) Gold, L. *J. Chem. Phys.* **1958**, *28*, 91.
(15) We have assigned the morphology of SI(0.64,1.12)-9 as perforated lamellae (P); however, coexisting lamellae (L) and poorly ordered hexagonally packed cylinders (C) is also a possibility consistent with our scattering results. The PL morphology was predicted by Matsen to remain metastable in polydisperse block copolymer melts as it is in the monodisperse case.[29]
(16) Fetters, L. J.; Lohse, D. J.; Richter, D.; Witten, T. A.; Zirkel, A. *Macromolecules* **1994**, *27*, 4639.
(17) Witzke, D. R.; Narayan, R.; Kolstad, J. T. *Macromolecules* **1997**, *30*, 7075.
(18) Rosedale, J. H.; Bates, F. S. *Macromolecules* **1990**, *23*, 2329.
(19) For PEP−PLA, the T_{ODT} represents the average of the three measurements of T_{ODT} during heating scans and three measurements of T_{ODT} during cooling scans. For PS−PI, T_{ODT} represents the average of three measurements during heating scans; the ODT upon cooling occurred slowly and appeared continuous on the experimental time scale (1 °C/min).
(20) Schmidt, S. C.; Hillmyer, M. A. *J. Polym. Sci., Part B: Polym. Phys.* **2002**, *40*, 2364. In addition to the synthesis of PEP−PLA, Schmidt and Hillmyer determined the interaction parameter ($\chi_{PEP-PLA}$) by measuring the temperature at the order−disorder transition for several symmetric PEP−PLA diblock copolymers and comparing to the mean-field prediction $(\chi N)_{ODT} \approx 10.5$ from: Leibler, L. *Macromolecules* **1980**, *13*, 1602.
(21) Khandpur, A. K.; Förster, S.; Bates, F. S.; Hamley, I. W.; Ryan, A. J.; Bras, W.; Almdal, K.; Mortensen, K. *Macromolecules* **1995**, *28*, 8796. χ_{PS-PI} used in determining the PS−PI phase diagram was obtained from: Rounds, N. A. Ph.D. Dissertation, University of Akron, 1970. Rounds used a ternary blend of PS−PI/PS/PI and measured the turbidity temperature as a function of blend composition, extrapolated to pure PS−PI to obtain the critical temperature for the pure diblock copolymer, and compared the results to a thermodynamic theory for microphase separation to determine χ_{PS-PI} (Meier, D. J. *J. Polym. Sci., Part B: Polym. Symp.* **1969**, *26*, 81).
(22) A more refined expression for χ_{PS-PI} may be found in ref 27. However, we have chosen to use χ_{PS-PI} from ref 21 to facilitate comparison with the published PS−PI phase diagram.
(23) A detailed description of the scattering observed in the perforated lamellar phase can be found in: Hamley, I. W.; Castelletto, V.; Mykhaylyk, O. O.; Yang, Z.; May, R.; Lyakhova, K. S.; Sevink, G. J. A.; Zvelindovsky, A. V. *Langmuir* **2004**, *20*, 10785. A detailed study of its metastability can be found in: Hajduk, D. A.; Takenouchi, H.; Hillmyer, M. A.; Bates, F. S.; Vigild, M. E.; Almdal, K. *Macromolecules* **1997**, *13*, 3788.
(24) Matsen, M. W. *Eur. Phys. J. E* **2006**, *21*, 199.
(25) Jiang, Y.; Huang, R.; Liang, H. *J. Chem. Phys.* **2005**, *123*, 124906. The free energy well about the minimum becomes shallower as the PDI is increased. See Figure 10 of ref 6 for another example as calculated by SCFT.
(26) Sakamoto, N.; Hashimoto, T.; Han, C. D.; Kim, D.; Vaidya, N. Y. *Macromolecules* **1997**, *30*, 1621. Sakamoto, N.; Hashimoto, T. *Macromolecules* **1998**, *31*, 8493. Han, C. D.; Vaidya, N. Y.; Kim, D.; Shin, G.; Yamaguchi, D.; Hashimoto, T. *Macromolecules* **2000**, *33*, 3767.
(27) Dormidontova, E. E.; Lodge, T. P. *Macromolecules* **2001**, *34*, 9143.
(28) Wang, J.; Wang, Z.-G.; Yang, Y. *Macromolecules* **2005**, *38*, 1979.
(29) Matsen, M. W. *Phys. Rev. Lett.*, in press.
(30) A fundamental difference between the PL and SI systems should be noted: the same poly(ethylene-*alt*-propylene) block was used in all PL diblock copolymers, and the polyisoprene block in each SI block copolymer was the result of a different polymerization; thus, the PDI is not perfectly constant among all SI samples. In all cases, the properties of the SI samples are correlated with the PS block PDI. The increased entropic cost of stretching the PS block over the PI block based on statistical segment lengths likely causes the effects of PDI to be more sensitive to changes in the PS-block PDIs than the PI-block PDIs.[16]
(31) Pangborn, A. B.; Giardello, A.; Grubbs, R. H.; Rosen, R. K.; Timmers, F. J. *Organometallics* **1996**, *15*, 1518.

MA070962R